Journal of Inflammation Research

Dovepress
open access to scientific and medical research

Open Access Full Text Article

ORIGINAL RESEARCH

Expansion of a Novel Subset of L-Selectin$^+$ Classical Monocytes in Kawasaki Disease

Yihua Jin[1,*], Zhimin Geng[1,2,*], Kun Lin[1], Xinyu Gu[1], Xiwei Feng[1], Songling Fu[1], Wei Wang[1], Chunhong Xie[1], Yujia Wang[1], Fangqi Gong[1]

[1]Department of Cardiology, Children's Hospital, Zhejiang University School of Medicine, National Clinical Research Center for Child Health, Hangzhou, People's Republic of China; [2]Pediatric Cardiovascular Diseases Laboratory, Children's Hospital, Zhejiang University School of Medicine, National Clinical Research Center for Child Health, Hangzhou, Zhejiang, People's Republic of China

*These authors contributed equally to this work

Correspondence: Fangqi Gong; Yujia Wang, Email gongfangqi@zju.edu.cn; wangyujia@zju.edu.cn

Purpose: Kawasaki disease (KD) is an acute systemic vasculitis that is associated with dysregulated immune responses. Monocytes play a central role in innate immunity. Our previous single-cell RNA sequencing of peripheral blood mononuclear cells (PBMC) revealed a new subset of monocytes in children with KD called L-Selectin$^+$ classical monocytes (SELL$^+$ CM). Therefore, we aimed to investigate the correlation between KD and SELL$^+$ CM.

Patients and Methods: Peripheral blood samples were collected from 81 KD patients, 18 febrile patients and 36 healthy children before treatment. Among them, ten KD patients were followed up, and samples were obtained before and after intravenous immunoglobulin (IVIG) treatment. Analysis of SELL$^+$ CM was performed using flow cytometry. Additionally, ROC curve analysis was conducted to assess the diagnostic value of SELL$^+$ CM for KD.

Results: Classical monocytes (CM) expressed the highest levels of L-selectin in children with KD. The ratio of SELL$^+$ CM in CM was significantly higher in KD patients than in febrile and healthy children. Following IVIG treatment, the ratio of SELL$^+$ CM in CM showed a downward trend. The receiver operating characteristic (ROC) curve analysis (the area under the curve, AUC = 0.71) indicated the potential diagnostic value of SELL$^+$ CM in KD. The correlation analysis suggested that SELL$^+$ CM may serve as a new clinical index for patients with KD.

Conclusion: In KD, the ratio of SELL$^+$ CM in CM significantly increases during the acute phase, which may become a potential biomarker and help facilitate KD diagnosis based on clinical features.

Keywords: Kawasaki disease, monocyte subsets, L-Selectin, coronary artery lesions

Introduction

Kawasaki disease (KD) has become the leading cause of acquired heart disease in children since it was first described in 1967 as a new mucocutaneous lymph node syndrome. KD causes acute vasculitis of the small- and medium-sized vessels, predominantly affecting the coronary arteries. The most severe sequela of KD is the induction of long-term cardiovascular complications such as coronary artery dilation, stenosis, aneurysms, occlusion and infarction.[1] In the intervening 55 years, efforts have been made to determine its etiology. Hypotheses range from viral etiologies to toxin-mediated reactions to autoinflammatory disease.[2] The most prevailing paradigm is that KD results from an infectious agent that elicits hyperinflammatory responses in genetically predisposed hosts, presented as vasculitis directed at cardiovascular tissues.[3] However, how the exaggerated inflammatory response in KD translates into vascular damage is still an enigma.

Though the etiology is complex, accumulating evidence has shown that immunological abnormalities are pivotal in acute-phase KD.[4] Among immune cells that are involved in the pathogenesis of KD, monocytes represent 10% of leukocytes in human blood and participate in vascular inflammation including vasculitis and atherosclerosis as well.[5,6]

Received: 6 May 2024
Accepted: 7 August 2024
Published: 9 September 2024

On the basis of modern nomenclature, there are three distinct subsets of human blood monocytes: Classical $CD14^{+}CD16^{-}$ monocytes (CM), Intermediate $CD14^{++}CD16^{+}$ monocytes (IM) and Nonclassical $CD14^{+}CD16^{++}$ monocytes (NCM).[7] An increase of $CD14^{++}CD16^{+}$ monocytes in KD patients during the acute stage has also been demonstrated.[8] However, most studies of KD did not stratify for monocyte subsets, and exploration of the actual role of each subtype of monocyte is needed. Based on our previous outcome of single-cell RNA-sequencing, $SELL^{+}$ CM, which was characterized by the expression of SELL, was locked in patients with KD.[9] It was the first time that $SELL^{+}$ CM was identified in KD. This study aimed to explore the association between KD and this monocyte subtype.

Selectins are a family of cell-surface molecules that mainly modulate the activity of leukocytes and platelets during immune responses.[10] Encoded by the gene SELL. L-Selectin (CD62L, originally LAM-1/LECAM-1) is a member of the selectin family, which has been found in most circulating leukocytes and is extensively considered a tethering/rolling receptor. Evidence also shows that L-selectin plays a role in guiding free-flowing monocytes from the bloodstream toward the surrounding extravascular environment during transendothelial migration (TEM).[11]

To further understand the exact role of $SELL^{+}$ CM in KD pathogenesis, augmenting the sample size of patients with KD is needed to clarify the correlation between $SELL^{+}$ CM and KD. Peripheral blood mononuclear cells (PBMC) were collected from 81 KD patients, 18 febrile control subjects (FC) and 36 healthy control subjects (HC). $SELL^{+}$ CM is upregulated in the acute phase of KD compared to that in the other two groups. These results suggest that $SELL^{+}$ CM may facilitate KD diagnosis.

Materials and Methods

Participants and Ethics

All patients with KD enrolled in this study were admitted to the Children's Hospital, Zhejiang University School of Medicine, between December 2022 and October 2023. Eighteen age- and gender-matched febrile patients were enrolled as febrile controls, including those with bronchopneumonia or pneumonia, upper respiratory infection and urinary tract infection. And 36 children who underwent routine physical examinations were recruited as healthy control. KD was diagnosed according to the American Heart Association criteria.[12] All the patients underwent physical and laboratory examinations. Two-dimensional echocardiography was performed during the acute and convalescent disease phases. Each hospitalized patient received 2 g/kg intravenous immunoglobulin (IVIG) and 30–50 mg/kg/day aspirin as the initial treatment. Patients who had other diseases or had been previously treated were excluded.

Peripheral blood samples (2 mL each) from 81 KD patients, 18 febrile patients and 36 healthy children were collected into tubes containing EDTA as an anticoagulant. As for KD patients, blood samples were collected during the acute phase before IVIG and corticosteroid treatment. The study was conducted in accord with the Declaration of Helsinki. The parents or guardians of the participants signed an informed consent form to participate in this study. This study was approved by the Institutional Review Board of Children's Hospital, Zhejiang University School of Medicine (IRB number: 2019-IRB-073).

Clinical Features

Demographic data, including sex and age at disease onset, were summarized. Data on early clinical presentation and laboratory findings, such as white blood cell count, C-reactive protein level (CRP), and erythrocyte sedimentation rate (ESR), were collected at diagnosis. Intravenous immunoglobulin resistance was defined as persistent or recrudescent fever at least 36h after completion of the first IVIG infusion.[12] The coronary artery abnormalities were classified according to the maximum Z scores for the right and left anterior descending coronary arteries: no involvement ($Z < 2$), dilation only ($Z \geq 2$ to < 2.5), and aneurysm ($Z \geq 2.5$).[12]

Flow Cytometry Analysis

Peripheral blood mononuclear cells were isolated using Ficoll-Paque PLUS (GE Healthcare Biosciences AB) according to the manufacturer's protocol. Briefly, 4 mL diluted peripheral blood sample (diluted with 2 mL phosphate-buffered saline) was carefully layered onto a 3 mL Ficoll-Paque media solution. After centrifugation at 400 × g for 30 min at

19°C, the mononuclear cell layer was obtained and washed twice with phosphate-buffered saline. The samples were cryopreserved in liquid nitrogen.

Using flow cytometry, L-Selectin^{+} classical monocytes were analyzed in PBMC as described and validated previously.[13] Detection of all samples from enrolled subjects has technical replicates for three times. Mononuclear cells were thawed and suspended in Stain Buffer (FBS, BD Pharmingen^{TM}). The cells were stained with APC-conjugated anti-human CD14, BV421-conjugated Anti-human CD16, PE-conjugated anti-human CD62L or their isotype controls (BD Biosciences), which were APC-conjugated mouse IgG2a (κ Isotype Control), PE-conjugated mouse IgG1 (κ Isotype Control), and BV421-conjugated mouse IgG1 (κ Isotype Control). Flow cytometry was performed using a BD FACSLyric Flow Cytometer equipped with a BD FACSuite (BD Biosciences). The results were analyzed using the FlowJo flow cytometry software (BD Biosciences, version 10.8.1). The mean fluorescence intensity (MFI) of L-Selectin on monocytes is summarized in Supplementary Figure 1.

Statistical Analysis

Data management and statistical analyses were performed using IBM SPSS Statistics (SPSS Inc., Chicago, Illinois, version 23) and GraphPad Prism (GraphPad Software, San Diego, CA, USA, version 9.5.1). Statistical significance was set at $p < 0.05$. Demographic data and clinical features were presented as medians with interquartile ranges (IQR). Other data are expressed as mean ± standard deviation (SD) from triplicate technical replicates. The independent *t*-test for normally distributed data and Mann–Whitney test for non-normally distributed data were used to compare the two groups. ANOVA for normally distributed data and Kruskal–Wallis test for non-normally distributed data were used when more than two variables were compared. The area under the curve (AUC) of the receiver operating characteristic (ROC) curve was used to evaluate the diagnostic value of SELL^{+} CM. Correlation analysis and visualization were performed using R programming language (version 3.1.5).

Results

Characteristics of Human Subjects

Demographic Data

A total of 81 KD patients, 18 sex-and age-matched FCs and 36 HCs were recruited for this study. The demographic characteristics of the study population are shown in Table 1. Among the patients with KD, 53 (65%) were male and 28 (35%) were female. The median age of patients with KD patients was 2.4 years, and the interquartile range (IQR) was 1.3 to 3.5. The maximum age was 9.5 years, and the minimum age was 0.3 years. In addition, no significant differences were observed in sex or age among the three groups.

Clinical Presentation and Laboratory Findings

The clinical and laboratory findings of the KD and FC patients were summarized in Table 2. In KD, the most common clinical manifestations were fever (86.42%), cervical lymphadenopathy (93.83%), and conjunctival infections (86.84%). Only 43.21% of the patients had extremity changes, and 61 (75.31%) patients presented with a polymorphous rash during the course of the disease. After completion of the first infusion of intravenous immunoglobulin, the persistent or recrudescent

Table 1 The Demographic Data of Human Subjects

Characteristics	KD Patients (n=81)	Healthy Controls (n=36)	Febrile Controls (n=18)	p value
Gender n (%)				NS
Male	53 (65)	17 (47)	12 (67)	
Female	28 (35)	19 (53)	6 (33)	
Age (years)				NS
Median (IQR)	2.4 (1.3 to 3.5)	3.4 (2.4 to 4.5)	3.6 (0.5 to 6.1)	
Minimum	0.3	0.4	0.1	
Maximum	9.5	6.6	8.1	

Abbreviations: KD, Kawasaki disease; IQR, Interquartile range.

Table 2 Clinical Presentation and Laboratory Results of KD and Febrile Patients

Clinical Presentation	KD Patients (n=81)	KD-CAL Patients (n=8)	IVIG-NR Patients (n=10)	Febrile Controls (n=18)
Physical findings				
Fever persisting for ≥5 days	70 (86.42%)	7 (87.50%)	8 (80%)	NA
Polymorphous rash	61 (75.31%)	5 (62.50%)	8 (80%)	NA
Oral mucosal changes	69 (85.19%)	2 (25.00%)	8 (80%)	NA
Conjunctival injection	70 (86.42%)	8 (100.00%)	8 (80%)	NA
Extremity Changes	35 (43.21%)	3 (37.50%)	4 (40%)	NA
Cervical lymphadenopathy	76 (93.83%)	8 (100.00%)	10 (100%)	NA
IVIG resistance	10 (12.35%)	0 (0)	-	NA
Coronary artery outcome				
Normal (Z<2)	73 (90%)	-	10 (100%)	NA
Dilation (Z≥2 to <2·5)	4 (5%)	4 (50%)	-	NA
Aneurysm (Z≥2·5)	4 (5%)	4 (50%)	-	NA
Laboratory results				
White blood cells, $10^3/\mu L$	13.2 (10.8 to 16.5)	11.2 (8.4 to 16.9)	12.3 (9.8 to 17.9)	13.7 (8.8 to 17.8)
Percentage of neutrophils	67.7 (56.1 to 77.4)	71.9 (52.0 to 75.6)	72.3 (54.4 to 85.2)	63.3 (54.6 to 69.6)
Percentage of monocytes	6.4 (4.6 to 8.2)	7.9 (5.2 to 10.2)	6.2 (5.4 to 7.2)	8.4 (6.4 to 10.3)
Platelets, $10^3/\mu L$	348 (286 to 419)	390 (330 to 462)	308.5 (266.8 to 383.3)	314 (260 to 399)
Haemoglobin, g/L	112 (105 to 118)	110 (107 to 114)	119 (109 to 121)	110 (104 to 121)
C-reactive protein, mg/dL	49.0 (29.3 to 87.0)	57.1 (20.0 to 96.9)	43.8 (30.2 to 91.7)	56.8 (39.0 to 86.9)
Erythrocyte sedimentation rate, mm/h	58.1 (42.2 to 73.5)	58.6 (42.5 to 100.9)	56.4 (37.8 to 67.4)	31.3 (21.0 to 52.4)
BNP, pg/mL	386.4 (109.1 to 855.6)	230.4 (113.0 to 725.1)	611.3 (123 to 1396.8)	40.5 (9.0 to 90.1)
Alanine transaminase, U/L	26 (15 to 85)	25 (13 to 37)	23 (19 to 137)	12 (9 to 17)
Gamma-glutamyl transferase, U/L	18 (13 to 75)	19 (13 to 142)	18 (11 to 189)	14 (11 to 27)
Total bilirubin, mg/dL	6.3 (5.0 to 10.3)	6.5 (4.4 to 40.2)	9.6 (4.0 to 26.6)	6.3 (4.9 to 8.8)

Notes: Data are presented as n, n/N (%), or median (IQR).
Abbreviation: *Z* scores, Body surface area-adjusted *Z* scores of coronary artery internal diameter measures.

fever of 71 patients with KD returned to normal, and the incidence of IVIG resistance was 12.35%. Despite timely treatment with IVIG and acetylsalicylic acid (ASA), the incidence of coronary artery lesions was 9.88% in the acute and subacute stages, including 4 (5%) patients with coronary artery dilation and 4 (5%) with aneurysm formation. Regarding laboratory outcomes, the median value of absolute counts for total white blood cells (WBC) was $13.2\times10^3/\mu L$ (10.8 to 16.5) and the increase in neutrophils in peripheral blood was the main cause of this phenomenon. Meanwhile, CRP, ESR, and BNP levels were significantly elevated in patients with KD. Other laboratory results of KD and FC patients were listed in Table 2.

L-Selectin Expression in Monocytes of KD Patients

A heatmap from flow cytometry demonstrated the discovery of L-Selectin in patients with KD (Figure 1A). To elucidate this phenomenon, SELL protein levels of the three monocyte subsets were analyzed. In most enrolled KD patients, CM had the highest ratio of SELL-positive cells, whereas NCM had the lowest ratio. The proportions of $SELL^+$ CM in the CM, IM, and NCM groups were 53%, 49.3%, and 37.2%, respectively (Figure 1B).

Higher Proportion of $SELL^+$ CM in KD Patients

Intriguingly, there was a remarkable expansion of $SELL^+$ CM in 81 KD patients when compared with febrile and healthy controls, and the difference was statistically significant (Figure 2A). And there was no difference between febrile patients and healthy controls (Figure 2A). Furthermore, we analyzed the levels of $SELL^+$ CM in patients with coronary artery lesions (CAL) as well as IVIG-resistant patients solely. As shown in the histogram, those with CAL exhibited a lower ratio of $SELL^+$ CM in the early stage of KD ($p = 0.0073$, Figure 2B). However, no obvious difference was found between the IVIG-resistant and IVIG-responsive patients (Figure 2C).

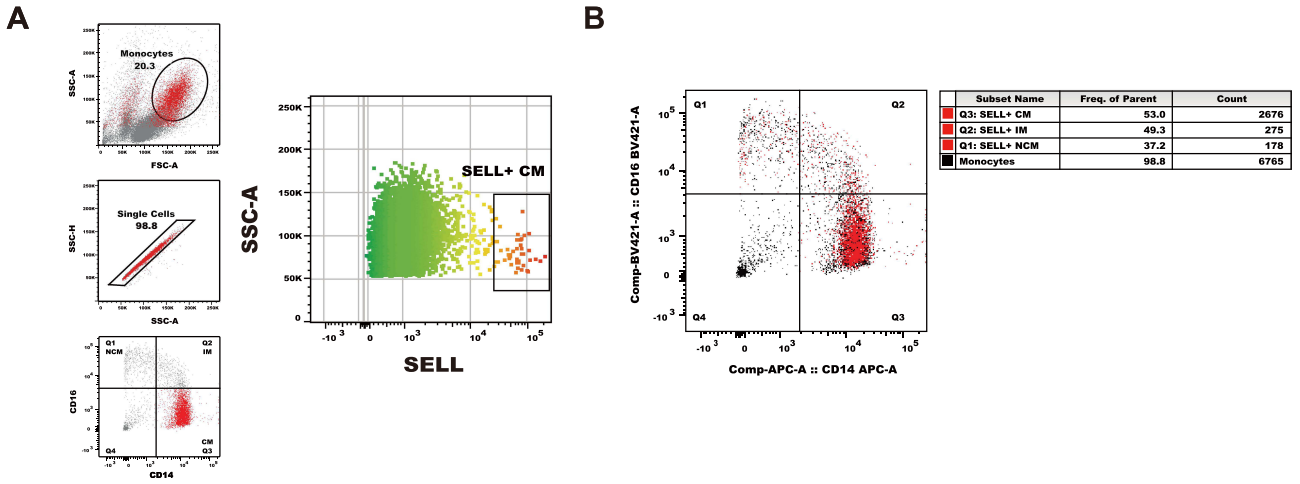

Figure 1 L-Selectin Expression in Monocyte Subsets. (**A**) Gating method for identifying SELL$^+$ CM (L-Selectin$^+$ classical monocytes). The left three squares indicate the labeling process of CM. The Orange dots in the square frame on the right represent SELL$^+$ CM. (**B**) Expression of SELL (L-Selectin) in different monocyte subsets: CM (classical CD14$^+$CD16$^-$ monocytes), IM (intermediate CD14^{++}CD16$^-$ monocytes), and NCM (nonclassical CD14$^+$CD16^{++} monocytes). The red dots represent SELL$^+$ cells. The frequencies of SELL$^+$ cells are summarized in the right chart.

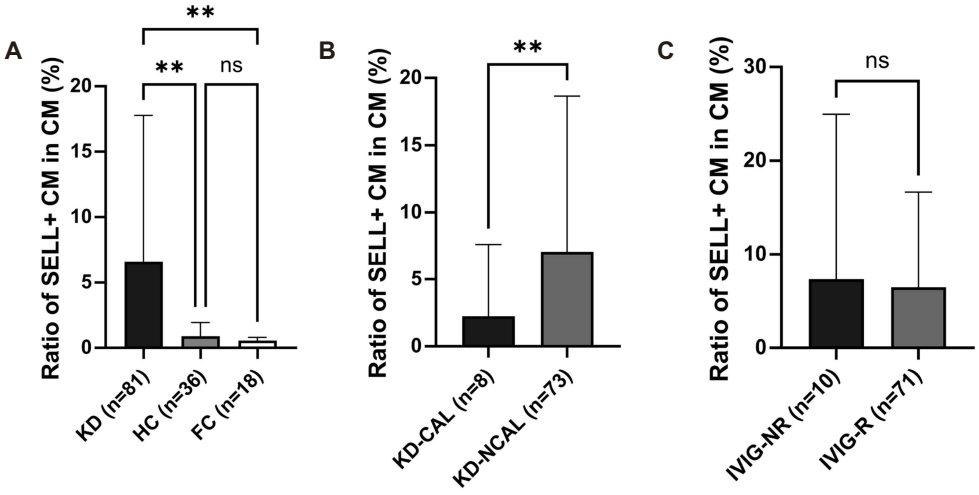

Figure 2 Comparison of SELL$^+$ CM Levels between Different Groups. (**A**) Comparison of the ratio of SELL$^+$ CM in CM among KD patients (n=81), FC (n=18) and HC (n=36). (**B**) Comparison of the ratio of SELL$^+$ CM between KD patients with coronary artery lesions (KD-CAL) (n=8) and KD patients without coronary artery lesions (KD-NCAL) (n=73). (**C**) Comparison of the ratio of SELL$^+$ CM between IVIG non-responsive (IVIG-NR) patients (n=10) and IVIG responsive (IVIG-R) patients (n=71). Statistics were performed using the Mann–Whitney test. ns: p>0.05. **: p<0.01.

The Variation Tendency of SELL$^+$ CM Level in KD

Among the 81 patients with KD, we followed up ten of them, including two patients diagnosed with coronary artery dilation. Patients were enrolled if their peripheral blood had been obtained before treatment and after the end of IVIG treatment. The results for the ten individuals are plotted in a line chart. High SELL$^+$ CM ratio persisted after IVIG treatment in the two patients in whom coronary artery lesions developed. However, SELL$^+$ CM ratio declined in 8 treated patients without coronary artery lesions (Figure 3).

ROC Curve and Correlation Analysis of SELL$^+$ CM in KD

To determine the ability of SELL$^+$ CM ratio to distinguish KD patients with febrile and healthy children, ROC curve analysis was used to assess its diagnostic performance. The results are presented in Figure 4A, indicating that SELL$^+$ CM performed well in distinguishing KD from common febrile diseases and healthy children, with an AUC of 0.71. To further figure out the role of SELL$^+$ CM in KD, a heatmap was generated to visualize the correlation between the SELL$^+$

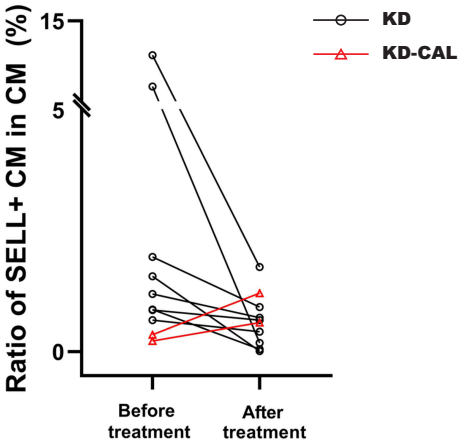

Figure 3 The variation tendency of SELL$^+$ CM ratio in KD patients before and after treatment.

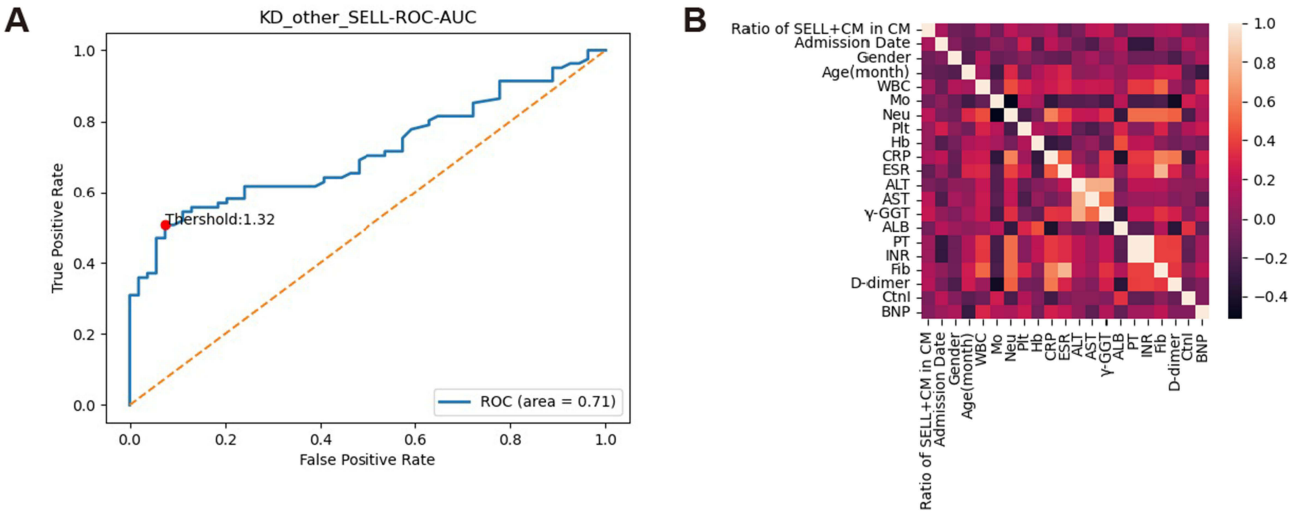

Figure 4 ROC Curve and Correlation Analysis of SELL$^+$ CM in KD. (**A**) ROC curve analysis of SELL$^+$ CM in KD patients (AUC = area under the curve). (**B**) Correlation matrix. The color bars indicate the degree of correlation between laboratory results and SELL$^+$ CM. The colors range from black (negative correlation) to pink (positive correlation). The intensity of the color represents the strength of the correlation between variables.

CM ratio and laboratory results (Figure 4B). However, our data showed a poor correlation between SELL$^+$ CM and laboratory characteristics.

Discussion

Prompt diagnosis of KD and timely prediction of coronary artery lesions are important for improving the prognosis. Prior studies have proposed candidate biomarkers for contributing acute KD diagnosis. Though not enough to lead decision-making, they still have certain value in differentiating KD. Elevations of NT-proBNP and sST2 are correlated with impaired myocardial relaxation in acute KD patients,[14] but the plasma and serum for NT-proBNP and sST2 detection are limited in young infants and children. Proteomic analysis of serum from KD patients revealed a panel of proteins potentially facilitate KD diagnosis;[15] however, serum proteome was affected by genetic backgrounds and environmental factors. Comparing with previous indicators, we focused on the diagnostic value of SELL$^+$ CM in KD. However, a large sample size and multi-centers are still needed to validate its value in clinical applications. We identified an upregulation of SELL$^+$ CM in KD patients when compared to febrile and healthy controls. Patients with CAL showed lower levels of SELL$^+$ CM in the acute phase. After the end of IVIG treatment, there was a downregulation of SELL$^+$ CM in KD-NCAL patients, whereas SELL$^+$ CM continued to increase in KD-CAL patients. The continuous variation of SELL$^+$ CM

changed obviously after IVIG treatment, which may also have some prognostic value. Several studies have demonstrated the mobilization of monocytes/macrophages during the exaggerated inflammatory response in KD.[8,16,17] The new exploration of $SELL^+$ CM sheds light on the role of monocytes in KD pathogenesis. Moreover, detection of $SELL^+$ CM levels may help KD diagnosis.

The obvious expansion of $SELL^+$ CM in the peripheral blood potentially enhances the invasive behavior of monocytes in patients with KD. New mounting evidence suggests that L-Selectin is a major player in regulating monocyte protrusion during transendothelial migration[18] and will be shed rapidly from monocytes upon activation (termed L-Selectin shedding).[19] Advanced imaging techniques show that inhibition of L-Selectin shedding significantly potentiates monocytes invasive behavior across activated endothelial cell monolayers.[11] This may account for the phenomenon that KD is an acute vasculitis, which may do damage to all the medium-sized arteries. L-Selectin shedding during rolling interaction physiologically limits the aggregation and accumulation of leukocytes.[20] In the present study, the retention of L-Selectin further amplified the abnormal activation of the immune system in KD.

The analysis showed a lower $SELL^+$ CM ratio in the patients with KD-CAL. Among the 81 patients, 8 children suffered from coronary artery lesions. In mammals, "Inflammatory monocytes" are featured with L-Selectin whereas "resident monocytes" are known for their patrolling behavior of vasculature and lack the expression of L-Selectin, they, respectively, correspond to human CM and NCM.[21,22] Most of the time monocytes circulate in the vasculature and will be recruited to sites when inflammation response happen.[23] In our study, the "inflammatory monocytes" in KD-CAL patients may tend to mature into "resident one" which are featured with patrolling behavior of blood vessels. It has been verified that L-Selectin plays a central role in mediating monocyte attachment to activated aortic endothelial cells.[24] Possibly, the vascular endothelium of KD-CAL patients was highly activated and flowing monocytes slowed down and recruited to inflamed endothelial monolayers. Therefore, the $SELL^+$ CM ratio was lower in peripheral blood of 8 KD-CAL patients. Meanwhile, L-Selectin shedding rapidly from leukocytes upon their activation. Comparing with KD-NCAL patients, the lower L-Selectin expression may reflect an augmented activation of leukocytes.[25] It has also been suggested that the downregulated cell surface expression of L-Selectin is due to extensive rolling of leukocytes on inflammatory endothelium. No wonder why $SELL^+$ CM from peripheral blood was found lower in KD-CAL patients. The prediction or timely diagnosis of CAL helps improve the prognosis of patients with KD. Further augmentation of KD-CAL samples is needed to verify whether a lower level of $SELL^+$ CM can aid in the diagnosis of coronary artery lesions.

After treatment, there was a decrease in the cell surface expression of L-selectin in KD-NCAL patients. Children with coronary artery lesions developed seemed to have persistent $SELL^+$ CM ratio increased. Albeit poorly understood, IVIG is the mainstream treatment for KD. The mechanisms by which IVIG treatment successfully led to a lowering of $SELL^+$ CM ratio are unknown. An elegant in vivo study showed that IVIG treatment has direct inhibitory effects on leukocyte adhesion and subsequent emigration, which leads to decreased vascular permeability and can reduce vascular dysfunction.[26] A second potential possibility is that IVIG infusion decreases inflammatory monocytes in vivo.[27] Moreover, IVIG has the ability to induce autophagy of inflammatory cells like monocytes and M1 macrophages.[28] As for KD-CAL, IVIG seemed to fail to decrease leukocyte and did not reduce their negative function to vascular.

Approximately 10–20% of KD patients are IVIG non-responsive and have a higher possibility of developing CAL.[29] Identifying IVIG non-responders is also necessary. The ratio of $SELL^+$ CM in CM between the IVIG nonresponsive and IVIG-responsive groups was compared, but there was no notable discrepancy between the two groups. Further studies are required to determine whether $SELL^+$ CM plays a role in the course of IVIG-resistant.

In the absence of pathognomonic laboratory tests, the diagnosis of KD still relies on recognition of clinical presentations. As a potential assist for discriminating KD from other diseases, the ROC curve analysis was performed to assess the diagnostic value of $SELL^+$ CM. The AUC value corroborates that this new finding may aid in the prompt diagnosis of KD. Finally, although numerous demographic and laboratory data were collected, no strong correlation was found between these indices and the $SELL^+$ CM level. This finding implies that $SELL^+$ CM may be a new clinical index for KD.

Our study had some limitations. First, only 8 patients with coronary artery lesions and only 10 patients who were non-responsive to IVIG were enrolled, which possibly led to poor statistical power. Second, exploration of the exact function

of SELL$^+$ CM in the mechanism of KD is still required. We intend to enrich and refine our experimental design to demonstrate the role of this new subset of monocytes in KD.

Conclusion

We identified a new subset of L-selectin$^+$ classical monocytes in KD children. Additionally, we confirmed the diagnostic value of SELL$^+$ CM in KD for the first time. This finding may help KD diagnosis and reveal a new pathogenesis of KD.

Acknowledgments

We acknowledge all participants involved in this study.

Funding

This work was supported by grants from the Key R&D Program of Zhejiang (2024C03179), National Natural Science Foundation of China (grant number: 82200551), and the China Postdoctoral Science Foundation (certificate number: 2023M733076).

Disclosure

The authors report no conflicts of interest in this work.

References

1. Cohen E, Sundel R. Kawasaki disease at 50 years. *JAMA Pediatr*. 2016;170(11):1093–1099. doi:10.1001/jamapediatrics.2016.1446
2. Lo MS. A framework for understanding Kawasaki disease pathogenesis. *Clin Immunol*. 2020;214:108385. doi:10.1016/j.clim.2020.108385
3. Noval Rivas M, Lee Y, Wakita D, et al. CD8+ T cells contribute to the development of coronary arteritis in the lactobacillus casei cell wall extract-induced murine model of Kawasaki disease. *Arthritis Rheumatol*. 2017;69(2):410–421. doi:10.1002/art.39939
4. Kumrah R, Vignesh P, Rawat A, Singh S. Immunogenetics of Kawasaki disease. *Clin Rev Allergy Immunol*. 2020;59(1):122–139. doi:10.1007/s12016-020-08783-9
5. Watanabe R, Hashimoto M. Pathogenic role of monocytes/macrophages in large vessel vasculitis. *Front Immunol*. 2022;13:859502. doi:10.3389/fimmu.2022.859502
6. Rahman MS, Murphy AJ, Woollard KJ. Effects of dyslipidaemia on monocyte production and function in cardiovascular disease. *Nat Rev Cardiol*. 2017;14(7):387–400. doi:10.1038/nrcardio.2017.34
7. Ziegler-Heitbrock L, Ancuta P, Crowe S, et al. Nomenclature of monocytes and dendritic cells in blood. *Blood*. 2010;116(16):e74–80. doi:10.1182/blood-2010-02-258558
8. Katayama K, Matsubara T, Fujiwara M, Koga M, Furukawa S. CD14+CD16+ monocyte subpopulation in Kawasaki disease. *Clin Exp Immunol*. 2000;121(3):566–570. doi:10.1046/j.1365-2249.2000.01321.x
9. Geng Z, Tao Y, Zheng F, et al. Altered monocyte subsets in Kawasaki disease revealed by single-cell RNA-sequencing. *J Inflamm Res*. 2021;14:885–896. doi:10.2147/jir.S293993
10. Purdy M, Obi A, Myers D, Wakefield T. P- and E- selectin in venous thrombosis and non-venous pathologies. *J Thromb Haemost*. 2022;20(5):1056–1066. doi:10.1111/jth.15689
11. Rzeniewicz K, Newe A, Rey Gallardo A, et al. L-selectin shedding is activated specifically within transmigrating pseudopods of monocytes to regulate cell polarity in vitro. *Proc Natl Acad Sci*. 2015;112(12):E1461–70. doi:10.1073/pnas.1417100112
12. McCrindle BW, Rowley AH, Newburger JW, et al. Diagnosis, treatment, and long-term management of Kawasaki disease: a scientific statement for health professionals from the American Heart Association. *Circulation Apr*. 2017;135(17):e927–e999. doi:10.1161/cir.0000000000000484
13. Furukawa S, Matsubara T, Yabuta K. Mononuclear cell subsets and coronary artery lesions in Kawasaki disease. *Arch Dis Child*. 1992;67(6):706–708. doi:10.1136/adc.67.6.706
14. Sato YZ, Molkara DP, Daniels LB, et al. Cardiovascular biomarkers in acute Kawasaki disease. *Int J Cardiol*. 2013;164(1):58–63. doi:10.1016/j.ijcard.2011.06.065
15. Kato T. Using biomarkers to predict unresponsiveness to initial immunoglobulin for Kawasaki disease patients. *Circ J*. 2022;86(6):984–985. doi:10.1253/circj.CJ-21-0821
16. Menikou S, Langford PR, Levin M. Kawasaki disease: the role of immune complexes revisited. *Front Immunol*. 2019;10:1156. doi:10.3389/fimmu.2019.01156
17. Takahashi K, Oharaseki T, Yokouchi Y. Pathogenesis of Kawasaki disease. *Clin Exp Immunol*. 2011;164(Suppl 1(Suppl 1)):20–22. doi:10.1111/j.1365-2249.2011.04361.x
18. Ivetic A, Hoskins Green HL, Hart SJ. L-selectin: a major regulator of leukocyte adhesion, migration and signaling. *Front Immunol*. 2019;10:1068. doi:10.3389/fimmu.2019.01068
19. Cappenberg A, Margraf A, Thomas K, et al. L-selectin shedding affects bacterial clearance in the lung: a new regulatory pathway for integrin outside-in signaling. *Blood*. 2019;134(17):1445–1457. doi:10.1182/blood.2019000685
20. Rahman I, Collado Sánchez A, Davies J, et al. L-selectin regulates human neutrophil transendothelial migration. *J Cell Sci*. 2021;134(3) doi:10.1242/jcs.250340
21. Geissmann F, Jung S, Littman DR. Blood monocytes consist of two principal subsets with distinct migratory properties. *Immunity*. 2003;19(1):71–82. doi:10.1016/s1074-7613(03)00174-2

22. Hamon P, Loyher PL, Baudesson de Chanville C, Licata F, Combadière C, Boissonnas A. CX3CR1-dependent endothelial margination modulates Ly6C(high) monocyte systemic deployment upon inflammation in mice. *Blood*. 2017;129(10):1296–1307. doi:10.1182/blood-2016-08-732164
23. Ruder AV, Wetzels SMW, Temmerman L, Biessen EAL, Goossens P. Monocyte heterogeneity in cardiovascular disease. *Cardiovasc Res*. 2023;119(11):2033–2045. doi:10.1093/cvr/cvad069
24. Giuffrè L, Cordey AS, Monai N, Tardy Y, Schapira M, Spertini O. Monocyte adhesion to activated aortic endothelium: role of L-selectin and heparan sulfate proteoglycans. *J Cell Biol*. 1997;136(4):945–956. doi:10.1083/jcb.136.4.945
25. Shimada Y, Sato S, Hasegawa M, Tedder TF, Takehara K. Elevated serum L-selectin levels and abnormal regulation of L-selectin expression on leukocytes in atopic dermatitis: soluble L-selectin levels indicate disease severity. *J Allergy Clin Immunol*. 1999;104(1):163–168. doi:10.1016/s0091-6749(99)70128-4
26. Jang JE, Hidalgo A, Frenette PS. Intravenous immunoglobulins modulate neutrophil activation and vascular injury through FcγRIII and SHP-1. *Circ Res*. 2012;110(8):1057–1066. doi:10.1161/circresaha.112.266411
27. Cavaliere FM, Prezzo A, Conti V, et al. Intravenous immunoglobulin replacement induces an in vivo reduction of inflammatory monocytes and retains the monocyte ability to respond to bacterial stimulation in patients with common variable immunodeficiencies. *Int Immunopharmacol*. 2015;28(1):596–603. doi:10.1016/j.intimp.2015.07.017
28. Das M, Karnam A, Stephen-Victor E, et al. Intravenous immunoglobulin mediates anti-inflammatory effects in peripheral blood mononuclear cells by inducing autophagy. *Cell Death Dis*. 2020;11(1):50. doi:10.1038/s41419-020-2249-y
29. Ye Q, Gong FQ, Shang SQ, Hu J. Intravenous immunoglobulin treatment responsiveness depends on the degree of CD8+ T cell activation in Kawasaki disease. *Clin Immunol*. 2016;171:25–31. doi:10.1016/j.clim.2016.08.012